ELSEVIER

Spectrochimica Acta Part B 63 (2008) 349–353

SPECTROCHIMICA ACTA PART B

www.elsevier.com/locate/sab

Compact fiber-optic fluorosensor employing light-emitting ultraviolet diodes as excitation sources ☆

Sara Ek, Benjamin Anderson [1], Sune Svanberg *

Atomic Physics Division, Lund University, P.O. Box 118, S-221 00 Lund, Sweden

Received 26 September 2007; accepted 12 November 2007
Available online 4 December 2007

Abstract

A compact fluorosensor using three different ultraviolet light-emission diodes as excitation sources for fiber-optic recording of fluorescence spectra from samples is described. A compact integrated spectrometer with linear array wavelength recording is used, yielding a spectral resolution of about 8 nm. In two system implementations ultraviolet light-emitting diodes at 300, 340 and 395 nm, or at 360, 385 and 410 nm were used as excitation sources with typical emission halfwidths of 12 nm, each combined with a matching long-path colored-glass filter automatically brought into the fluorescence light flow for suppression of reflected light. Spectra from measurements on vegetation, human skin tumors and a rare-earth ion-based thermographic phosphor were recorded to illustrate the system performance.

Keywords: UV light-emitting diode; Fluorescence; Spectrometer; Cancer diagnostic

1. Introduction

Fluorescence spectroscopy is a powerful diagnostic modality that complements reflectance spectroscopy in a large variety of non-intrusive, real-time applications including analytical chemistry, forensic sciences, environmental monitoring and medical diagnostics. In particular, laser-induced fluorescence has been applied in fiber-optic point monitoring as well as in multispectral imaging using a wide variety of systems. Applications to biomedicine have used fluorosensors such as the ones described in Refs. [1] and [2], and imaging systems as exemplified in Refs. [3] and [4]. Reviews can be found, e.g. in Refs. [5] and [6]. Laser-induced fluorescence can also be applied in a remote-sensing variety using fluorescence lidar techniques both for spectral recordings and for large-area imaging [7,8]. Fluorescence recordings are frequently performed with a spectrometer showing the full spectrum. However, the recorded spectrum is also strongly influenced by the excitation wavelength, and thus it is desirable to have multiple wavelengths in the excitation source. Nitrogen lasers operating at 337 nm have proved to be a convenient source for inducing fluorescence and a simple dye laser can be used to generate additional wavelengths (see, e.g. Ref. [1,2]). With the advent of blue and UV diode lasers through work at Nichia Corporation [9] a compact and convenient excitation source became available. A fluorosensor based on a 395 nm diode laser is described in Ref. [10]. With commercial diode lasers now available at as low wavelengths as 375 nm a fluorosensor with multiple-wavelength excitation could in principle be constructed. However, since such diode lasers are vulnerable to electrical transients combined with being costly, and very short wavelengths could anyway not be achieved, such a solution is less attractive. Observing that fluorescence spectra of liquids and solids are quite broad-banded and thus really do not require narrow-band excitation, it was instead realized, that multiple light-emitting diodes (LEDs) available for ultraviolet (UV) wavelengths down to 250 nm could instead be used.

A peculiarity in fluorescence diagnostics is that it is mandatory to block the strong excitation light by additional filtering,

☆ This article is published in a special honor issue dedicated to Jim Winefordner on the occasion of his retirement, in recognition of his outstanding accomplishments in analytical atomic and molecular spectroscopy.

* Corresponding author.
E-mail address: sune.svanberg@fysik.lth.se (S. Svanberg).
[1] Present address: Laser and Fibre-Optics Centre, University of Cape Coast, Cape Coast, Ghana.

0584-8547/$ - see front matter © 2007 Elsevier B.V. All rights reserved.
doi:10.1016/j.sab.2007.11.026

since the spectrometer/detector alone cannot handle the strong reflected light in the presence of the weak emission of interest; this is due to stray light, blooming etc. Thus, an individually matched long-pass filter has to be inserted in the detection light beam for each excitation source. A single filter cannot be used, since then it would have to match the longest wavelength LED. However, it is highly desirable to capture fluorescence as close to the excitation wavelength as possible, since here the strongest discriminative features frequently occur.

In finding an appropriate arrangement for the efficient use of multiple excitation sources we have evaluated pros and cons of different solutions (mechanical switching of the different LEDs in synchronism with switching filters using rotary stage or sledges and the use of reflecting optics (spherical or off-axis parabolas), placing the exchangeable filter outside or inside the spectrometer etc). Mechanically switchable LEDs can give better photon economy but need frequent mechanical adjustment which is less compatible with portable use. The present paper reports on the construction and performance of a novel fluorosensor largely based on fiber-optic components, and representative application examples are given.

2. Fluorosensor set-up

The general arrangements for our UV-LED-based fluorosensor are given in Fig. 1a and b. A photograph of the instrumentation is shown in Fig. 1c. In order to induce fluorescence at multiple excitation wavelengths two different arrangements, each with three different excitation wavelengths, produced in UV LEDs, were used. In one arrangement diodes with nominal operating wavelengths at 300 nm, 340 nm and 395 nm are used as light sources in the fluorosensor. The LEDs have integrated lenses made by UV-transmitting material, and three individual fibers of diameter 400 μm, optimally placed in the light flow, carrying excitation light from the UV diodes are merged into a single 400 μm fiber (A.R.T. Photonics GmbH). In an alternative arrangement, three LEDs with UV-transmitting epoxy lenses were used. Holes were drilled into the epoxy to accommodate the light-collecting fibers, which were thus placed in a pig-tailed arrangement with the fiber ends as close to the light-emitting chips as possible. We used a combination of 360, 385 and 410 nm diodes, 360 nm being the shortest-wavelength LED with machine-workable epoxy lens. The LEDs, all delivered by Roithner Laser Technique, are powered by batteries inside the fluorosensor and can be switched on and off on computer command. The fiber into which the three individual laser fibers were merged, and a further fiber connected to the spectrometer, are then merged into a single fiber of diameter 600 μm (Fig. 1a), the distal end of which is placed in contact with the object under study. The output light power at the fiber tip is a fraction of a mW and is completely eyesafe. Induced fluorescence is collected and guided back towards the fluorosensor via the same fiber, and at the first joint, part of it is transferred into the spectrometer fiber. Fluorescence spectra are recorded in an Ocean Optics USB4000 miniature spectrometer with a 3648 element CCD (Charged Coupled Device) array. The 200 μm spectrometer entrance slit results in about 8 nm resolution,

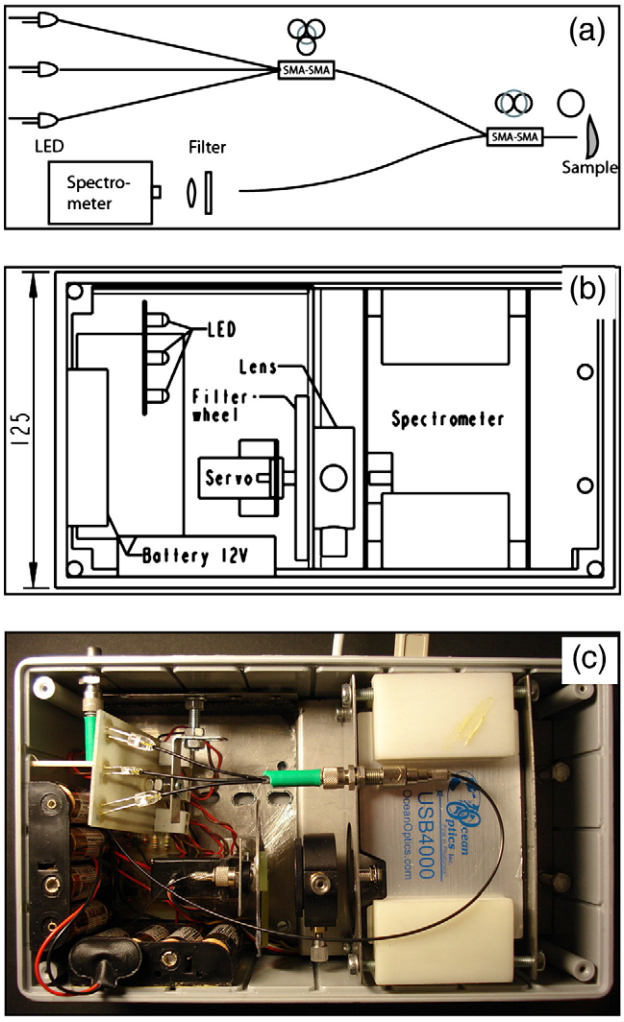

Fig. 1. (a) Optical scheme of the system with fiber couplings indicated. (b) Layout of the fluorosensor based on multiple UV-emitting diodes. Length of side: 125 mm. (c) Photograph of the system.

which is adequate for fluorescence monitoring. The elastically backscattered LED light is blocked by Schott colored-glass filters (WG320, GG385 for the first set of diodes, GG385 and GG455 for the second set of diodes) placed on a computer controlled filter wheel in front of a lens (UV Grade Fused Silica lens, Edmund Optics, $f = 13.5$ mm) focusing the fluorescence light onto the spectrometer slit. Individual long-pass filters are desired to ensure that fluorescence can be measured as close to the excitation wavelength as possible, since specific information on the target material frequently can be found here. However, the filter GG385 turned out to be the most efficient filter for filtering out the 385 and 395 nm excitation light as well.

A schematic overview of the spectral aspects of our fluorosensor is given in Fig. 2. Here the spectral profiles of the UV LEDs used in our first arrangement with matching long-pass filters are schematically shown together with experimental fluorescence spectra of chlorophyll and protoporphyrin IX, representative for environmental and biomedical applications, respectively. We note, that the comparatively broad fluorescence structures well match the finite widths of the LEDs. The

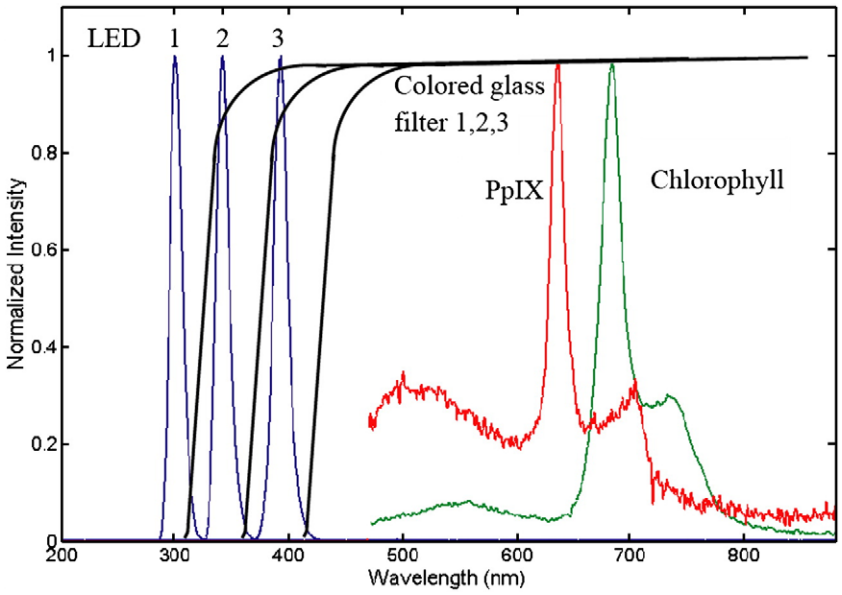

Fig. 2. Spectral characteristics of components of the fluorosensor and typical spectra.

spectra would basically have looked the same for narrow-band laser excitation. A special problem when using broad-band UV LEDs is that a long-wavelength tail tends to leak through the colored-glass filter, adding some reflectance light to the fluorescence light for short wavelengths. This signal can to first order be subtracted from the recorded spectrum; this has been done in the spectra shown in this paper. White light spectral correction was also applied to the data in Figs 4 and 5.

Autofluorescence induced in the optical fibers carrying the excitation light was found to have a negligible effect on the result but autofluorescence from the filters has to be subtracted. The comparatively long exposure time required makes the system sensitive for ambient light. However, since the optics is well shadowed inside the fluorosensor box and the fiber-optic probe is arranged to create a local shadow at the measuring site, the ambient light is effectively suppressed allowing measurements to be preformed in daylight.

Data-taking was fully controlled by LabVIEW computer code. Thus, a single-knob activation initiates a sequence, where first a background spectrum is recorded without any diode activated followed by sequential data-taking for each of the three LEDs being lit up and combined with the proper long-path filter, turned into the optical path in front of the spectrometer slit by rotating the filter wheel under computer control. The spectra could then be corrected to the case of a white spectral response of the fluorosensor by establishing a multiplicative spectral correction function. For this purpose spectral recordings through the measurements probe of the light from a 200 W calibrated quartz tungsten/halogen lamp (Oriel 63355) with a known spectral profile were recorded. The three corrected spectra are then displayed together, and further data processing, including e.g. multivariate analysis [11], can then be performed with the laptop computer, controlling the fluorosensor.

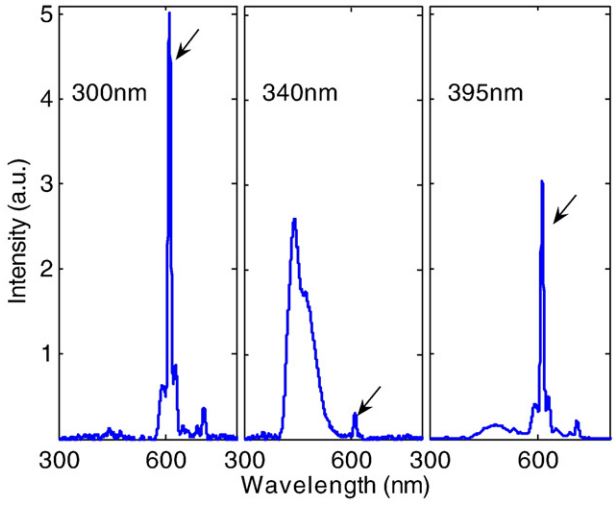

Fig. 3. Spectra from Y_2O_3:Eu^{3+}, excited at 300, 340 and 395 nm. It can be seen that the 611 nm line is very sensitive to the excitation wavelength. No spectral correction was applied.

3. Measurements

We have used the new compact instrument on different types of samples including thermographic phosphors, plants and human tumors.

3.1. Thermographic phosphor

The measurements made with the fluorosensor on a known thermographic phosphor [12], Europium-doped yttrium oxide (Y_2O_3:Eu^{3+}), shown in Fig. 3, clearly demonstrate that the fluorescence is strongly dependent on the excitation wavelength. The 300 nm LED is within the europium absorption band and should induce strong fluorescence at the emission line 611 nm. 340 nm, on the other hand, possesses the lowest

absorption value in the entire spectrum and will hardly induce any fluorescence at 611 nm. One of the strongest ionic transitions in this material is found at an excitation wavelength of 394.5 nm, perfectly matched to the LED at 395 nm.

3.2. Plant fluorescence

Chlorophyll *a* in green vegetation is effectively excited in the blue and red spectral regions yielding a dual-band spectral profile with peaks at about 685 and 740 nm [13]. Each specimen has its own spectroscopic finger-print, also considering accessory pigments and leave-coating wax, and after multivariate analysis different species may be spectroscopically identified. Fluorescence recordings from a field study in Ghana are shown in Fig. 4, where data from nutmeg and papaya leaves are shown.

3.3. Tumor fluorescence

When human skin is illuminated with a violet source the tissue autofluorescence ranges from blue to red with a maximum intensity around 460 nm. Several different fluorophores contribute to the autofluorescence, including elastin, collagen, NADH, and carotene. The average fluorescence intensity decreases in malignant lesions due to changes in chemical composition and hemoglobin absorption of the excitation light. A tumor sensitizer with characteristic fluorescence signature in the near infrared spectrum can be used for tumor identification and demarcation. The sensitizer protoporphyrin IX (PpIX) precursor δ-amino levulinic acid (ALA) is a natural constituent in the body, utilized as the starting material in the heme cycle. PpIX is produced at higher concentrations in diseased cells than in healthy areas. This photosensitizer is used in photodynamic therapy, a treatment that enables selective eradication of cancer cells.

The fluorosensor described was used in connection with tumor photodynamic therapy at the Oncology Clinic at the Lund University Hospital. Examples of spectra from normal tissue and tumor are shown in Fig. 5, displaying an increased 635 nm fluorescence due to PpIX in tumor. We note that 410 nm gives rise to the largest PpIX signal, since its largest absorption occurs at 405 nm.

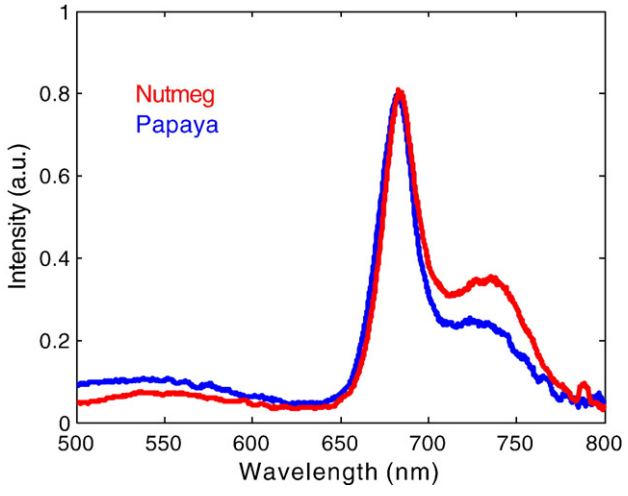

Fig. 4. Spectra from nutmeg and papaya leaves (Ghana). The excitation wavelength is 395 nm.

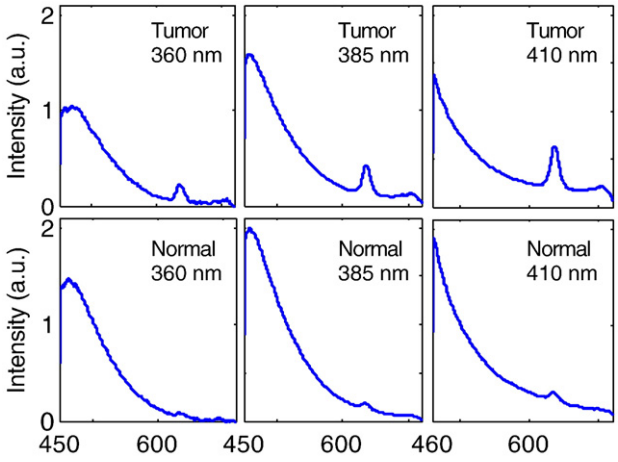

Fig. 5. Fluorescence spectra recorded for a basal cell carcinoma tumor and for normal surrounding skin. A cream containing δ-amino levulinic acid (ALA) had been applied to the area 4 h before the measurement, and PpIX has been synthesized to a higher degree in the tumor area as evidenced by the size of the 635 nm fluorescence peak. Three different excitation wavelengths were used: 360, 385 and 410 nm.

4. Discussion

A compact fiber-optic fluorosensor was constructed and the usefulness of multiple excitation wavelengths was demonstrated. Skin cancer diagnostics using PpIX fluorescence was demonstrated. Also the skin autofluorescence may provide valuable information about the patient status. Recently, the role of Advanced Glycation End (AGE) products as a possible major factor in aging and age-related chronic diseases, such as diabetes, Alzheimer's disease, atherosclerosis and chronic renal failure has been discussed (see, e.g. Ref. [14]). AGEs can accumulate in nearly every type of cells in the body and are produced when sugar and lipids react with proteins. Recently it was demonstrated that AGE can be measured in skin autofluorescence [15–18]. Several AGE components fluoresce at 440 nm when illuminated with 370 nm, why a fluorosensor in the UV region could be useful for the measurements. Preliminary measurements along these lines have been performed with the system, and multiple UV excitation wavelengths are of particular interest in this context.

The system performance is similar to what is obtained from single-wavelength diode-laser-based fluorosensors. The LEDs can readily be replaced with units emitting at other wavelengths. The general light collection efficiency of the present system is somewhat low, leading to several seconds of data integration time. However, higher LED output power and better fiber couplings/matching could realistically take down the spectral recording time to a second. Exact correction for the long-wavelength tail of the LEDs, leaking through the color-glass filter, as well as for the filter autofluorescence could be challenging in assuring true spectral shapes at short fluorescence

wavelengths. However, in practical diagnostics applications using multivariate analysis [11] with learning data sets, this potential problem is not important.

Acknowledgements

The authors gratefully acknowledge the friendly help from Mats Andersson and Linda Persson in setting up the system, Mikkel Brydegaard for assistance with programming, and the collaboration with J. Eghan, and Niels Bendsoe and K. Svanberg, in performing the plant and the clinical measurements, respectively. We also acknowledge fruitful discussions with S. Bengmark. This work was supported by the Swedish Research Council, the International Science Programme, Uppsala, and the Knut and Alice Wallenberg Foundation.

References

[1] S. Andersson-Engels, Å. Elner, J. Johansson, S.-E. Karlsson, L.G. Salford, L.-G. Strömblad, K. Svanberg, S. Svanberg, Clinical recording of laser-induced fluorescence spectra for evaluation of tumour demarcation feasibility in selected clinical specialities, Lasers Med. Sci. 6 (1991) 415–424.

[2] C. af Klinteberg, M. Andreasson, O. Sandström, S. Andersson-Engels, S. Svanberg, Compact medical fluorosensor for minimally invasive tissue characterization, Rev. Sci. Instr. 76 (2005) 1–6.

[3] S. Andersson-Engels, J. Johansson, S. Svanberg, Medical diagnostic system based on simultaneous multispectral fluorescence imaging, Appl. Opt. 33 (1994) 8022–8029.

[4] K. Svanberg, I. Wang, S. Colleen, I. Idvall, C. Ingvar, R. Rydell, D. Jocham, H. Diddens, S. Bown, G. Gregory, S. Montán, S. Andersson-Engels, S. Svanberg, Clinical multi-colour fluorescence imaging of malignant tumours — initial experience, Acta Radiologica 39 (1998) 2–9.

[5] S. Andersson-Engels, C. af Klinteberg, K. Svanberg, S. Svanberg, In vivo fluorescence imaging for tissue diagnostics, Phys. Med. Biol. 42 (1997) 815–824.

[6] T. Vo-Dinh, Biomedical Photonics Handbook, CRC Press LLC, New York, 2003.

[7] P. Weibring, H. Edner, S. Svanberg, Versatile mobile lidar system for environmental monitoring, Appl. Optics 42 (2003) 3583–3594.

[8] S. Svanberg, Fluorescence spectroscopy and imaging of Lidar targets, Chapter 7, in: T. Fujii, T. Fukuchi (Eds.), Laser Remote Sensing, CRC Press, Boca Raton, 2005, pp. 433–467.

[9] S. Nakamura, G. Fasol, The Blue Laser Diodes, Springer, Heidelberg, 1997.

[10] U. Gustafsson, S. Pålsson, S. Svanberg, Compact fiber-optic fluorosensor using a continuous-wave violet diode laser and an integrated spectrometer, Rev. Sci. Instr. 71 (2000) 3004–3006.

[11] K. Esbensen, T. Midtgaard, S. Schonkopf, D. Guyof, Multivariate Analysis — A Training Package, CAMO ASA, Oslo, 1994.

[12] S.W. Allison, D.L. Beshears, M.R. Cates, A.R. Bugos, The University of Tennesse — Knoxville TN, Martin Marietta Energy Systems — Oak Ridge TN.

[13] H.K. Lichtenthaler, U. Rinderle, The role of chlorophyll fluorescence in the detection of stress conditions in plants, CRC Crit. Rev. Anal. Chem. 19 (1988) S29–S85.

[14] S. Bengmark, Advanced glycation and lipoxidation end products — amplifiers of inflammation: The role of food, J. Parenteral and Enteral Nutrition 31 (2007) 430–440.

[15] R. Meerwaldt, R. Graaff, P.H.N. Oomen, T.P. Links, J.J. Jager, N.L. Alderson, S.R. Thorpe, J.W. Baynes, R.O.B. Gans, A.J. Smit, Simple non-invasive assessment of advanced glycation endproduct accumulation, Diabetologia 47 (2004) 1324–1330.

[16] R. Meerwaldt, T. Links, R. Graaff, S.R. Thorpe, J.W. Baynes, J. Hartog, R. Gans, A. Smit, Simple noninvasive measurement of skin autofluorescence, Ann. N.Y. Acad. Sci. 1043 (2005) 290–298.

[17] J.W.L. Hartog, A.P.J. de Vries, H.L. Lutgers, R. Meerwaldt, R.M. Huisman, W.J. van Son, P.E. de Jong, A.J. Smit, Accumulation of advanced glycation end products, measured as skin autofluorescence, in renal disease, Ann. N.Y. Acad. Sci. 1043 (2005) 299–307.

[18] G.N. Stamatas, R.B. Estanislao, M. Suero, Z.S. Rivera, J. Li, A. Khaiat, N. Kollias, Facial skin fluorescence as a marker of the skin's response to chronic environmental insults and its dependence on age, Photobiology 154 (2006) 125–132.